THE GAMMA-RAY SOURCE AGL J2241+4454 AS THE POSSIBLE COUNTERPART OF MWC 656

Pere Munar-Adrover[1], S. Sabatini[1,4], Giovanni Piano[1], Marco Tavani[1,4,5], L. H. Nguyen[2], F. Lucarelli[3,6], F. Verrecchia[3,6], and C. Pittori[3,6]

[1] INAF/IAPS-Roma, I-00133 Roma, Italy; pere.munar@iaps.inaf.it
[2] Institut für Experimentalphysik, Universität Hamburg, Germany
[3] ASI Science Data Centre (ASDC), via del Politecnico snc, I-00133 Roma, Italy

ABSTRACT

AGILE discovered the transient source AGL J2241+4454 in 2010, which triggered the study of the associated field allowing for the discovery of the first Be/black hole binary system: MWC 656. This binary was suggested to be the counterpart of AGL J2241+4454, but this association is still not robust. In this work we explore the archival *AGILE* and *Fermi*/Large Area Telescope (LAT) data to find more transient events compatible with AGL J2241+4454 and address the possibility to link them to the accretion/ejection processes of MWC 656. We found a total of nine other transient events with *AGILE* compatible with the position of AGL J2241+4454, besides the 2010 one. We folded these events with the period of the binary system and we could not associate the gamma-ray activity with any particular orbital phase. By stacking the 10 transient events we obtained a spectrum that extends between 100 MeV and 1 GeV, and we fitted it with a power law with a photon index $\Gamma = 2.3 \pm 0.2$. We searched the *Fermi*/LAT data in order to complement the gamma-ray information provided by *AGILE* but no significant results arose. To investigate this apparent contradiction between these telescopes, we studied the exposure of the field of AGL J2241+4454 in both instruments, and found significant differences. In particular, *AGILE* exposed, for a longer time and at a lower off-axis angular distance, the field of AGL J2241+4454. This fact, together with the energy-dependent sensitivity of both instruments, and the soft spectrum found in the stacking analysis, might explain why *AGILE* observed the transient events not seen by *Fermi*/LAT.

Key words: binaries: general – gamma-rays: stars – stars: black holes – stars: emission-line, Be – stars: individual (MWC 656) – X-rays: binaries

1. INTRODUCTION

In 2010 July the *AGILE* satellite detected a gamma-ray transient source, AGL J2241+4454, below the Galactic plane (Lucarelli et al. 2010), thus far from the strong diffuse Galactic emission. Within the *AGILE* position error box there are only four prominent X-ray sources: RX J2243.1+4441, a radio quasar (Brinkmann et al. 1997); HD 215325, an eclipsing binary of beta Lyr type (Kiraga & Stȩpień 2013); TYC 3226-1310-1, a rotationally variable star (Kiraga & Stȩpień 2013); and MWC 656, a massive Be star (van Leeuwen 2007). Both HD 215325 and TYC 3226-1310-1 star systems do not host the conditions for gamma-ray emission processes, such as accreting companions or the collision of two strong stellar winds, which could accelerate particles up to relativistic energies and thus produce gamma-rays. As we will show throughout the paper, we consider MWC 656 as the most likely candidate to be the counterpart of the gamma-ray transient emission.

MWC 656 has been recently discovered to be the first binary system containing a black hole (BH) and a Be companion star (Casares et al. 2014). This system was discovered thanks to its putative association with the transient gamma-ray source AGL J2241+4454 (Lucarelli et al. 2010) that triggered multi-wavelength observations.

This binary system is located at galactic coordinates $(l,\ b) = (100°.18,\ -12°.40)$ and shows a photometric

modulation of 60.37 ± 0.04 days (Williams et al. 2010; Paredes-Fortuny et al. 2012) which suggested its binary nature, confirmed by Casares et al. (2012). Phase zero, ϕ_0, is defined at the optical maximum (53242.8 MJD) and the periastron occurs at $\phi = 0.01 \pm 0.1$ (Casares et al. 2014). In the latter paper, it was found that the compact object is a BH with a mass between 3.8 and 6.9 $M_\odot$, and the Be star was reclassified as a B1.5-B2 III type star with a mass between 10 and 16 $M_\odot$. X-ray follow up observations revealed a faint X-ray source (Munar-Adrover et al. 2014) compatible with the position of the Be star, allowing for the classification of this system as a high-mass X-ray binary (HMXB). The X-ray spectrum was fitted with a blackbody plus a powerlaw model. The total X-ray luminosity in the 0.3–5.5 keV band is $L_X = (3.7 \pm 1.7) \times 10^{31}$ erg s^{-1}. The measured X-ray spectrum is dominated by the non-thermal component, with a non-thermal luminosity $L_{pow} = (1.6^{+1.0}_{-0.9}) \times 10^{31}$ erg s^{-1} $\equiv (3.1 \pm 2.3) \times 10^{-8} L_{Edd}$ for the estimated BH mass. This very low X-ray luminosity is compatible with the binary system being in quiescence during the X-ray observations and is at the level of the faintest low-mass X-ray binaries (LMXBs) ever detected, such as A0620−00 (Gallo et al. 2006) and XTE J1118+480 (Gallo et al. 2014). The non-thermal component is interpreted by Munar-Adrover et al. (2014) as the contribution arising from the vicinity of the BH and is studied in the context of the accretion/ejection coupling seen in LMXBs (Fender 2010), and also in the context of the radio/X-ray luminosity correlation (Corbel et al. 2013; Gallo et al. 2014).

[4] INFN Roma Tor Vergata, I-00133 Roma, Italy.
[5] Dip. di Fisica, Univ. Tor Vergata, I-00133 Roma, Italy.
[6] INAF-OAR, via Frascati 33, I-00040 Monte Porzio Catone, Italy.

Recent VLA radio observations by Dzib et al. (2015) showed that the binary system is also a weak radio source with variable emission. The peak of the radio flux density is $14.2 \pm 2.9\,\mu$Jy for a single $\sim$2 hr observation taken in 2015 February 22, at orbital phase $\sim$0.49, while six subsequent radio observations carried out during 2015 at the same sensitivity did not show any radio signal. However, stacking these other six observations yielded a detection with a flux density of $3.7 \pm 1.4\,\mu$Jy compatible with the position of MWC 656.

At TeV energies, MWC 656 was observed in 2012 and in 2013 with the MAGIC telescopes. The 2013 observations were contemporaneous to the *XMM-Newton* observation by Munar-Adrover et al. (2014). According to X-ray and optical data, these observations were thus performed during an X-ray quiescent state of the binary system and yielded only upper limits to its possible very high energy (VHE) emission at the level of $2.0 \times 10^{-12}\,\mathrm{cm}^{-2}\,\mathrm{s}^{-1}$ above 300 GeV (Aleksić et al. 2015).

X-ray binary (XRB) systems containing a Be star have been studied for a long time through radio and X-ray surveys. These systems are characterized by their variable X-ray emission and for their strong radio flares. Out of 184 known BeXRB systems, in 119 of them X-ray pulsations are observed, confirming that the compact component must be a neutron star (Ziolkowski 2014). In the remaining BeXRBs, the nature of the compact object is still unknown, with no confirmed BH known with a Be companion. This is known as the missing Be/BH binary problem (Belczynski & Ziolkowski 2009), and the predicted number of existing systems of this kind at any time is a few tens in our Galaxy (Grudzinska et al. 2015). In our case, the newly discovered MWC 656 system opens a new window in the study of this class of binaries. The missing Be/BH population could then possibly reveal itself through gamma-ray surveys more easily than with X-ray surveys and could have been subject to selection effects up to now.

In this work we present new *AGILE* and *Fermi*/Large Area Telescope (LAT) data analysis: we searched for persistent, transient and periodic emission at the position of MWC 656. We also discuss possible counterparts of the gamma-ray events and the possible association of the transient gamma-ray emission found with MWC 656 in the context of the accretion/ejection scenario.

2. THE MWC 656 FIELD

Although MWC 656 seems to be the most favoured candidate to produce the transient emission that has been detected by *AGILE*, we cannot discard another source as the counterpart.

In the vicinity of AGL J2241+4454 there is a *Fermi*/LAT source, 3FGL J2247.8+4413, which is identified with NVSS J224753+441317, a BL Lac object (Acero et al. 2015). It is located at galactic coordinates $(l, b) = (100°72, -13°25)$, at a distance of $0°93$ from the position of AGL J2241+4454. We considered this source at the time of analyzing *AGILE* data to take into account possible contamination. However, this is a very faint source with a flux of $F(E > 1\,\mathrm{GeV}) = (5.3 \pm 0.5) \times 10^{-10}\,\mathrm{cm}^{-2}\,\mathrm{s}^{-1}$ and variable behavior. Hence, in the short time periods when *AGILE* detected the transient emission the effect of 3FGL J2247.8+4413 on the detection is negligible.

The error box of the first *AGILE* transient detection is $1°2$ in diameter. As for X-ray emitting sources in the field, there is a known quasar near MWC 656, RX J2243.1+4441 (Brinkmann et al. 1997), which appears also in the X-ray images taken by Munar-Adrover et al. (2014). Quasars are also known to produce flaring activity at many wavelengths (Hartman et al. 2001) and this could be the case. However, there is little information about RX J2243.1+4441, its behavior and characteristics, due to the lack of optical counterpart and scarce radio and X-ray data. This source can be classified as a radio galaxy through its radio morphology (Marcote 2015): it presents a bright core at the center of the galaxy with a radio flux of 2.2 mJy beam^{-1}, stable over month timescales with faint signatures of a jet, and two radio lobes expanding toward the intergalactic medium spanning more than $50''$. However, the available radio data at only one frequency do not allow for a spectral characterization of the source. The radio morphology of this object resembles the classical FR-II type radio galaxies. While FR I-type radio galaxies have been found to emit in gamma-rays in several cases (Acero et al. 2015), FR-II type seem to be rarer in the GeV sky (Abdo et al. 2010; Grandi et al. 2012), disfavouring, although not excluding, RX J2243.1+4441 as the putative counterpart of AGL J2241+4454.

In the X-rays, a revision of the *XMM-Newton* data (Obs ID 0723610201), shows that the radio galaxy exhibits a spectrum with peak around 0.5 keV and fades away above 5 keV. The spectral fit with an absorbed power-law model yields a photon index $\Gamma = 1.8 \pm 0.4$ and a flux in the $0.2–5.0$ keV range of $F(0.2–5\,\mathrm{keV}) = (6.0 \pm 0.7) \times 10^{-14}\,\mathrm{erg\,cm}^{-2}\,\mathrm{s}^{-1}$. These results are roughly compatible within uncertainties with the Brinkmann et al. (1997) results using *ROSAT*-PSPC data. For a detailed view of the AGL J2241+4454 field see the Appendix.

For the above reasons, in the rest of the paper we consider MWC 656 as the most probable candidate counterpart of AGL J2241+4454.

3. OBSERVATIONAL DATA

3.1. AGILE Data

AGILE is a gamma-ray astrophysics mission operating since 2007 April (Tavani et al. 2008). It carries two main co-aligned instruments observing at hard X-rays between 18 and 60 keV (Super-*AGILE*, Feroci et al. 2007) and at high-energy (HE) gamma-rays between 30 MeV and 30 GeV (*AGILE*/GRID, Barbiellini et al. 2002; Prest et al. 2003). The instrumentation is completed by a calorimeter sensitive in the 0.4–100 MeV range (Labanti et al. 2006) and an anticoincidence detector (Perotti et al. 2006). *AGILE* has a wide field of view (FoV) of about 2.5 sr at HE gamma-rays and good sensitivity above 100 MeV. The point-spread function (PSF) at 100 and 400 MeV is $3°5$ and $1°5$ (68% containment radius), respectively (Sabatini et al. 2015). The sensitivity after one week of integration time in pointing mode is at the level of $20–30 \times 10^{-8}\,\mathrm{cm}^{-2}\,\mathrm{s}^{-1}$ above 100 MeV, depending on the off-axis angles and pointing directions (Tavani et al. 2008).

Since November 2009 *AGILE* has been observing in scanning mode, covering the whole sky every few hours. This observation mode allows for the study of serendipitous sources, such as AGL J2241+4454. Typical sensitivity in this observing mode is $\sim 10^{-7}\,\mathrm{cm}^{-2}\,\mathrm{s}^{-1}$ for 2 days integration time.
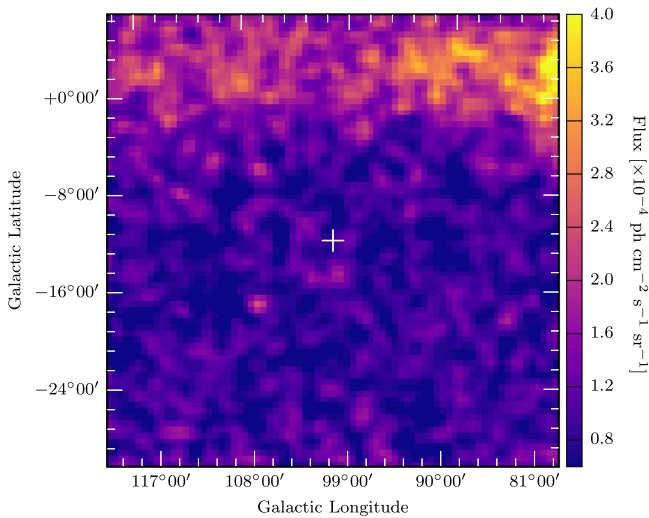
Figure 1. Deep *AGILE* pointing integration intensity map around the position of MWC 656 (white cross). The color-map represents a three-pixel kernel Gaussian smoothed number of counts. Pixel size is $0°2$.

Figure 2. *AGILE* two-day integration intensity map corresponding to data published in Lucarelli et al. (2010) at date 2010 July 25 (MJD 55402). The black ellipse represents the 95% c.l. containment of gamma-ray flux and the black cross marks the nominal position of the Be star MWC 656. The color-map represents a three-pixel kernel Gaussian smoothed number of counts, with a pixel size of $0°5$.

3.2. Fermi/LAT Data

The *Fermi* gamma-ray space telescope was launched in June 2008 and carries two main instruments: the LAT and the Gamma-ray Burst Monitor. The LAT is a non-homogeneous pair conversion tracker that works in the 30 MeV–300 GeV energy range and has a large collection area, ranging from 1000 to 5000 cm^2 for the front-LAT component. The instrument 68% containment radius ranges from $7°$ to $0°1$ in the considered energy range and the instrument angular resolution is optimized around 1 GeV (Sabatini et al. 2015). *Fermi*/LAT operates in scanning mode, monitoring continuously a wide part of the sky every few hours, with a typical sensitivity of 10^{-7} cm^{-2} s^{-1} for 1 day integration. Note that, due to the scanning observing mode, sources spend a very small amount of time (if any) on-axis.
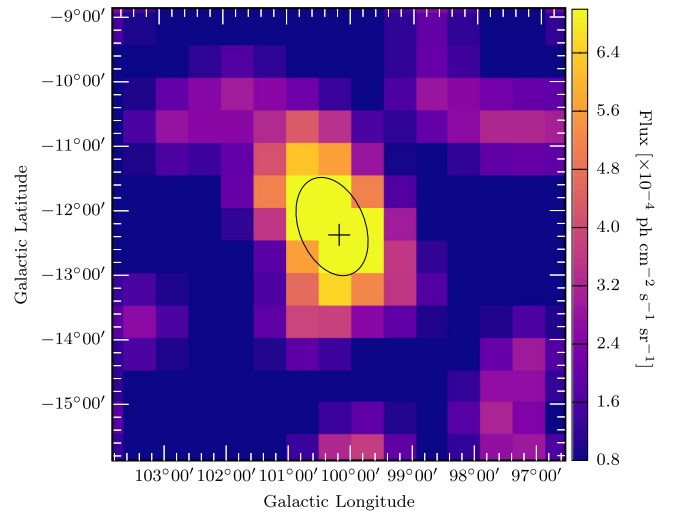
4. DATA ANALYSIS

4.1. AGILE Data Analysis

The analysis of gamma-ray data presented in this work was carried out with the *AGILE*/GRID FM3.119I0023 Build22 calibrated filter with a gamma-ray event selection that takes into account South Atlantic Anomaly event cuts and $80°$ Earth albedo filtering. Throughout the work, statistical significance assessment and source flux determination were established using the standard *AGILE* multi-source likelihood analysis software (Chen et al. 2012). The method provides an assessment of the statistical significance in terms of a test statistic (TS) defined as in Mattox et al. (1996) and asymptotically distributed as a $\chi^2/2$ for three degrees of freedom ($\chi^2_3/2$).

4.1.1. Search for Persistent Gamma-ray Emission

A search for persistent gamma-ray emission has been conducted over the public *AGILE* consolidated archive available from the ASI Science Data Center[7] at the time of the analysis, which covered observations up to the end of 2013.

We performed a multi-source likelihood analysis above 100 MeV of the $\sim$7 years of *AGILE* data; no detection has arisen so far and an upper limit at the level of $UL(E > 100 \text{ MeV}) = 2 \times 10^{-9}$ cm^{-2} s^{-1} has been obtained. We do not expect to find persistent gamma-ray emission in this system since XRBs spend most of their time in a quiescent state (Plotkin et al. 2013). During this state there is no presence of a radio jet, or it is not powerful enough to accelerate particles up to HE, and hence the possibility of producing inverse Compton (IC) and/or pion decay emission is remote. In Figure 1 we show a wide FoV intensity map with a long integration time where the AGL J2241+4454 is not visible and its position is marked with a white cross.

4.1.2. Search for Transient Gamma-ray Emission

In 2010 July 27 the *AGILE* team reported transient gamma-ray activity detected from an unidentified source at galactic coordinates $(l, b) = (100°0, -12°2)$ during the period 2010 July 25 01:00—2010 July 26 23:30 UT (Lucarelli et al. 2010). A refined maximum likelihood analysis of this transient event yields a 5.3σ detection with a flux of $F(E > 100 \text{ MeV}) = (2.0 \pm 0.7) \times 10^{-6}$ cm^{-2} s^{-1}. Figure 2 shows the intensity map above 100 MeV for this event.

After the gamma-ray detection in 2010 and the discovery of MWC 656 as a Be/BH binary system in a position compatible with AGL J2241+4454, a search for transient emission at other epochs has been performed. A blind search multi-source likelihood analysis around the position of AGL J2241+4454 for energies above 100 MeV has been conducted in two-day bins with no overlap between them, yielding a total of 10 gamma-ray transient or flaring events at a position compatible, within their 95% position uncertainties, with the one reported in Lucarelli et al. (2010), and with the position of MWC 656. These transient events spread from 2007 up to 2013, including both pointing and spinning observations, and the details about each one are displayed in

---

Table 1
AGILE Gamma-ray Transient Detections around the Position of MWC 656

t_{start} (UT)	t_{end} (UT)	Flux ($\times 10^{-6}$ cm^{-2} s^{-1})	$\sqrt{TS}$
2007 Nov 23 UT00:00:00	2007 Nov 24 UT00:00:00	1.5 ± 0.5	4.5
2008 Jun 28 UT00:00:00	2008 Jun 30 UT00:00:00	0.6 ± 0.3	3.2
2009 Jan 04 UT00:00:00	2009 Jan 07 UT00:00:00	0.5 ± 0.2	3.1
2010 Jun 13 UT00:00:00	2010 Jun 14 UT00:00:00	1.4 ± 1.1	3.2
2010 Jun 30 UT00:00:00	2010 Jul 02 UT00:00:00	1.3 ± 0.6	3.1
2010 July 25 UT00:00:00	2010 Jul 27 UT00:00:00	1.4 ± 0.6	5.3
2011 Apr 09 UT00:00:00	2011 Apr 11 UT00:00:00	2.2 ± 1.1	3.1
2011 Oct 08 UT00:00:00	2011 Oct 10 UT00:00:00	2.5 ± 1.1	3.4
2013 Aug 07 UT00:00:00	2013 Aug 08 UT00:00:00	2.6 ± 1.4	3.1
2013 Jul 10 UT00:00:00	2013 Jul 12 UT00:00:00	3.2 ± 1.6	3.5

Table 1. In this table we list the peak position of the transient emission, in galactic coordinates, the date and time of the starting and ending of the transient events, the flux and the significance as $\sqrt{TS}$. In Figure 4 we show the flux of these detections plotted over time, in MJD units, toghether with the significance of each one. A total of 151 and 758 two-day bins were analyzed for pointing and spinning observations, respectively.

Given that the significance of most of the events found is only a little above 3σ, we computed the probability of these detections to be by chance using the procedure explained in Bulgarelli et al. (2012). With this method we computed the probability of having k detections—consistent with the position of AGL J2241+4454, and hence with MWC 656 —with a significance $\sqrt{TS} \geqslant \sqrt{h}$ with N trials, which is given by:

$$P(N, k) = 1 - \sum_{j=0}^{k-1} \binom{N}{j} p^j (1 - p)^{N-j},$$

where p is the p-value corresponding to h which, for a detection significance $\sqrt{TS} \geqslant 3$ for a source below the Galactic plane whose counterpart might be known, is $p = 1.3 \times 10^{-3}$. For the $N = 909$ two-day bins in which we searched for transient events the probability of the 10 detections being by chance is $P(909, 10) = 6.8 \times 10^{-7}$, which translates into 4.97 Gaussian standard deviations. Given this probability and the fact that the detections are always compatible with the position of MWC 656, we think that it might be reasonable to consider the 10 detected events as true transient gamma-ray emission.

With this result in mind, a stacked analysis of the 10 detections was carried out and yielded a best position for our source of interest of $(l, b) = (100°37, -12°39) \pm 0°35$. The spectrum, which is displayed in Figure 3, was binned into four channels, 100–200, 200–400, 400–1000 and 1000–3000 MeV, and was fitted with a power law obtaining a photon index $\Gamma = 2.3 \pm 0.2$. The overall significance for this stacked analysis is $\sqrt{TS} = 8.9$.

4.1.3. Search for Periodic Gamma-ray Emission

Since the gamma-ray transient AGL J2241+4454 has been proposed to be the counterpart of MWC 656 we have conducted a search for periodicity in the gamma-ray flares detected by *AGILE*. We have folded the transient detections

with the period of MWC 656, in accordance with the Casares et al. (2014) ephemeris, and these are displayed in Figure 7. The detected flares span between phase 0 and 0.8 approximately, leaving a small gap without any gamma-ray detection. There is no evident periodic behavior in the gamma-ray emission from AGL J2241+4454 that might be associated with MWC 656. This kind of emission, however, was not expected, since the orbital parameters of the system seem to point at a very small eccentricity (Casares et al. 2014).

4.2. Fermi/LAT Data Analysis

For the purpose of this work, we used the Science Tools provided by the *Fermi* satellite team[8] on the Pass8 data around the position of AGL J2241+4454. The version of the Science Tools used was `v9r33p0` with the P8R2_TRAN-SIENT010_V6 instrument response function (IRF). The reader is referred to *Fermi* instrumental publications for further details about IRFs and other calibration details (Ackermann et al. 2012).

We have adopted the current Galactic diffuse emission model (`gll_iem_v06.fits`) in a likelihood analysis and `iso_P8R2_SOURCE_V6_v06.txt` as the isotropic model, and the *Fermi*/LAT third point source catalog `gll_psc_v16.fit` (Acero et al. 2015) has been used.[9] In the modelization of the data, the Galactic background and diffuse components remained fixed. We selected Pass8 FRONT and BACK transient class events with energies between 0.1 and 300 GeV. Among them, we limited the reconstructed zenith angle to be less than 105° to greatly reduce gamma-rays coming from the limb of the Earth's atmosphere. We selected the good time intervals (GTI) of the observations by excluding events that were taken while the instrument rocking angle was larger than 50°.
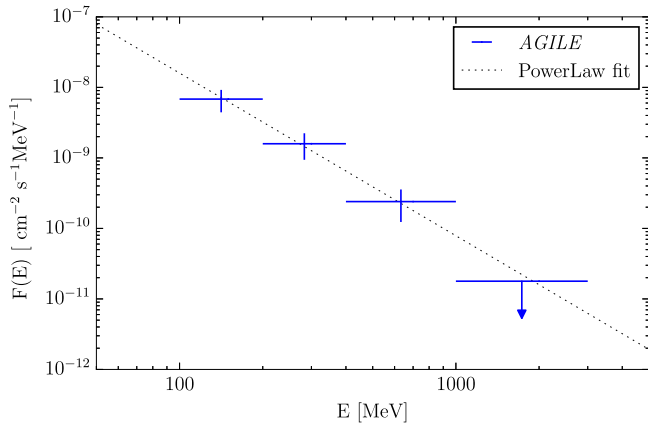
In the model for our source we used a power-law model for MWC 656 and used the `make3FGLxml.py` tool to obtain a model for the sources within 25° region of inrerest (ROI). To analyze the data we used the user contributed package *Enrico*.[10]

We divided each analisys into two steps: in the first one we leave all parameters of all the sources within a 10° ROI free,

---

[8] http://fermi.gsfc.nasa.gov
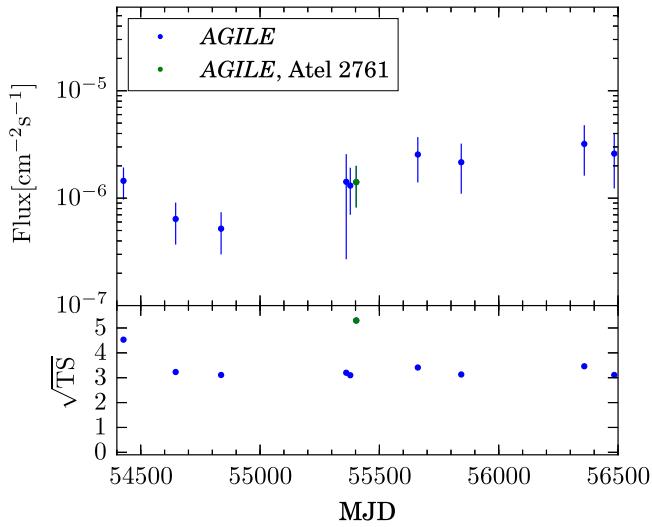[9] http://fermi.gsfc.nasa.gov/ssc/data/access/
[10] https://github.com/gammapy/enrico/

Figure 3. Photon spectrum between 100 MeV and 3 GeV of MWC 656 as detected by *AGILE*/GRID by integrating all flaring episodes in pointing and spinning mode. The dotted line represents the best power-law fit, with a photon index $\Gamma = 2.3 \pm 0.2$.

Figure 4. *AGILE* detections plotted over time. The green data point corresponds to the event published in Lucarelli et al. (2010).

while the sources outside this ROI up to 25° have their parameters fixed. Then we run a likelihood analysis using the Minuit optimizer, which determines the spectral-fit parameters, and obtain a fit for all these sources. In the second step, we fix all the parameters of the sources in our model to the fitted values, except for our source of interest, and run again the likelihood analysis with the Newminuit optimizer to obtain a refined fit. At all times, the central target source MWC 656 kept all its spectral parameters free.

A systematic search in the *Fermi*/LAT data was carried out searching for transient emission on two-day time integration bins, retrieving non-significant events. The time intervals of the eight *AGILE* flares during which *Fermi*/LAT was already operational were also searched and no detections arose, yielding upper limits at the level of a few $10^{-7}\,\mathrm{ph\,cm^{-2}\,s^{-1}}$. We stacked these eight time intervals in order to be more sensitive and performed an analysis that resulted also in a non-detection of the source, yielding an
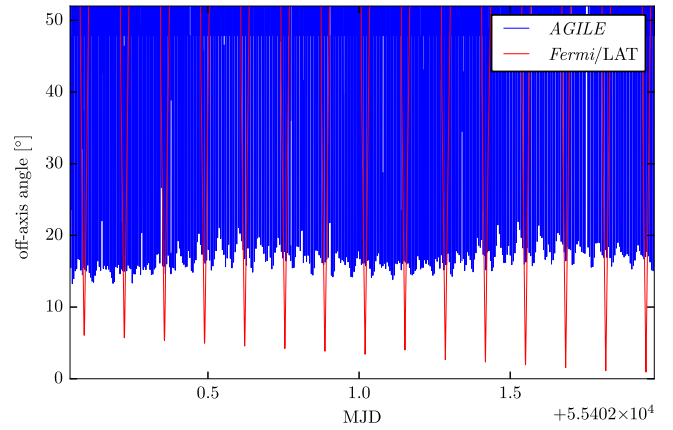

Figure 5. Time-evolution of the MWC 656 off-axis angles, as observed by *AGILE* and *Fermi*/LAT during the time interval reported by Lucarelli et al. (2010).

upper limit at the level of $3 \times 10^{-7}\,\mathrm{ph\,cm^{-2}\,s^{-1}}$ above 100 MeV. We also performed a search for periodic emission in the *Fermi*/LAT data by folding the data with the orbital period of 60.37 days of MWC 656. For this purpose we divided the orbit into eight bins to ensure having enough statistics and repeated the analysis procedure as explained. No detection arose at any particular orbital phase and upper limits were obtained at the level of $\sim 2 \times 10^{-9}\,\mathrm{ph\,cm^{-2}\,s^{-1}}$. In the next section we discuss the implications of these results.

4.2.1. Comparison between AGILE and Fermi/LAT Data

Given the distinct results found by both gamma-ray telescopes we wanted to investigate why this had happened, as it is not the first time that one event has been seen only by one of these telescopes (see for instance Sabatini et al. 2013). It is important to note that the detectability of transient emission for a specific source depends on the effective area (larger by a factor 5–10 in *Fermi*/LAT compared to *AGILE* depending upon energy in the range 100 MeV–1 GeV, and decreasing with off-axis angle for both instruments), on the effective time on source (depending on the observation mode, which is different in the two telescopes) and marginally on the spectral energy distribution of the emission (with *AGILE* optimized in the 100–400 MeV channel and *Fermi*/LAT optimized for higher energies).
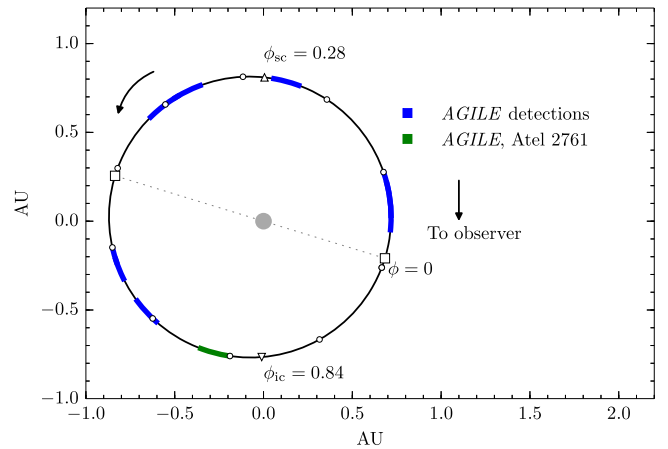
For example, Figure 5 shows the time evolution of the source off-axis angle—i.e., the angular distance between MWC 656 and the FoV center—for each instrument, during the event detected by *AGILE* on 2010 July 25 (Lucarelli et al. 2010). We can note that—most of the time—the source is inside the *AGILE*-GRID FoV at small off-axis angles, whereas it transits at large off-axis angles (or outside the FoV) in *Fermi*/LAT: MWC 656 is observed at angular distance lower than 50° in 41% of the total time for *AGILE* and 25% for *Fermi*/LAT. It is important to remark that, at high values of the off-axis angle (>50°), the sensitivity of *Fermi*/LAT is poor with respect to the nominal on-axis value (50% smaller).
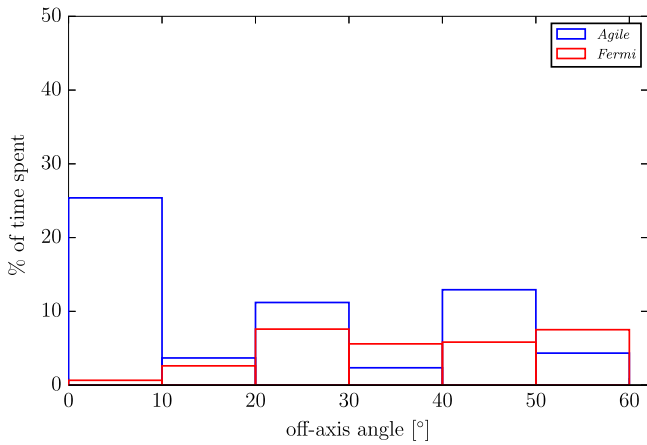
Figure 6. *AGILE* and *Fermi*/LAT histograms for the off-axis angle of MWC 656 during all the detected transient events.

Figure 7. Sketch of the orbit of MWC 656 according to the ephemeris from Casares et al. (2014). The *AGILE*-detected transient events are plotted on top. Squares mark the position of the periastron and the apastron whereas triangles mark the position of inferior and superior conjunctions. The orbit of the BH, the size of the star and the duration of the *AGILE* observations are scaled to the real values.

The other time intervals of transient emission detected by *AGILE* are also marginally exposed by *Fermi*/LAT and Figure 6 shows the fraction of time during which the source has been observed at a given interval of the off-axis angle by *AGILE* and *Fermi*/LAT during all the events in Table 1. *AGILE* has a much better angular exposition of the source with respect to *Fermi*/LAT. The low exposed *Fermi*/LAT observations, related to a reduced visibility of the source, provides a flux UL of $2.6 \times 10^{-8}\,\mathrm{cm}^{-2}\,\mathrm{s}^{-1}$ for the stacked analysis of all the events in Table 1, and typical ULs of the order of $\sim 9 \times 10^{-8}\,\mathrm{cm}^{-2}\,\mathrm{s}^{-1}$ for a two-day integration time. Thus, these values are not consistent with the *AGILE* results. However, these ULs are related to average gamma-ray emission during the two-day time intervals. Nevertheless, short radio flares, possibly related to the binary system activity, have been recently observed (Dzib et al. 2015). Therefore in the following we discuss the hypothesis that the flare duration is shorter than the integrated time.

A soft spectrum flare with a short duration of about ~ 3–$4\,\mathrm{hr}$ could have been seen by only one telescope if the arrival times of the (few) incident photons were within the GTI of that telescope. Alexander & McSwain (2015) studied the discrepancy between *AGILE* and *Fermi*/LAT. In their Figure 4, they show that, during the time intervals of higher *AGILE* count rates, *Fermi*/LAT was not in a GTI data-taking, and possibly lost most of the photons detected by *AGILE*. In order to discuss these cases, we carried out simulations of short transient emission with `gtobssim` (*Fermi*/LAT Science Tools). We simulated a source with the same flux as the average flux seen by *AGILE* in the 2010 event ($2.0 \times 10^{-6}\,\mathrm{ph}\,\mathrm{cm}^{-2}\,\mathrm{s}^{-1}$) and with the same spectral index ($\Gamma = 2.3$). The same attitude spacecraft file for real data was used in the simulation in order to use the exact positioning and GTIs of the satellite. To perform such a test, we assumed that the flare observed by AGILE lasted for a few hours and the flux that we obtained is diluted within the two-day integration time that was used in the analysis. Hence, we simulated a source with a higher flux than the observed, but lasting only 4–6 hr out of the total two-day simulated time interval, in order to have a realistic scenario. The results of this simulations with the *Fermi*/LAT Science Tools show that a short lived flare lasting for 4 or 6 hr would not be seen

by *Fermi*/LAT, obtaining a significance of 2σ and 3σ, and upper limits at the level of 1.1×10^{-7} and $2.0 \times 10^{-7}\,\mathrm{ph}\,\mathrm{cm}^{-2}\,\mathrm{s}^{-1}$, respectively.

5. DISCUSSION

The discovery of AGL J2241+4454 by *AGILE* has triggered a series of studies that led to the discovery of the first Be/BH binary system, MWC 656. However, the actual nature and counterpart of AGL J2241+4454 remains uncertain. The usual counterparts of flaring or transient gamma-ray events are blazars, novae and gamma-ray or X-ray binaries. However, the portion of the sky where AGL J2241+4454 was found seems to be poorly populated with these kinds of objects. The most suitable and also interesting candidate is still MWC 656.

Among the sources that can be found within the error box of AGL J2241+4454, we considered MWC 656 as the main candidate to be the counterpart of the gamma-ray activity. Within this assumption, we have plotted the gamma-ray transient events folded with the period of 60.37 days of this binary system (see Figure 7). We found that the transient emission is distributed along the orbit with no preferred orbital phase for the gamma-ray activity, i.e., there is no clustering of the detections at any particular phase. At some of these orbital phases the compact object is behind the Be star (see Figure 7). Other binary systems, like Cygnus X-3, have been found to emit in gamma-rays (Tavani et al. 2009; *Fermi*/LAT Collaboration et al. 2009). The modulated gamma-ray emission shows a bright maximum at the superior conjunction (where the compact object is behind the donor star). This behavior can be explained by assuming a simple leptonic scenario (anisotropic efficiency of the IC scattering, Dubus et al. 2010), or a hadronic scenario with an anisotropic or clumpy wind (Sahakyan et al. 2014).

The orbit of the binary system is almost circular, with an eccentricity of 0.10 ± 0.04 (Casares et al. 2014). With such a low eccentricity, there is almost no difference between the periastron and apastron passages, and thus the interaction

between the compact object and the donor star is expected to be almost steady in time. A possible source of variability within the system might be instabilities in the accretion disk around the BH and/or variations in the strong equatorial wind of the Be star. Hubert & Floquet (1998) observed that rapid variability in the optical emission in Be stars occurred more often in early-type Be stars, as is the case of MWC 656. If this variability occurs in this binary and it affects the accretion regime onto the BH, this might explain the gamma-ray transient events.

MWC 656 has been recently classified as an HMXB (Munar-Adrover et al. 2014) and during the X-ray observation in 2013 the source exhibited a very low luminosity, compatible with a quiescent state. The recent VLA radio detections by Dzib et al. (2015) showed variable radio emission with a peak at a flux density of $14.2 \pm 2.9\,\mu$Jy for a single ~2 hr observation at orbital phase ~0.5. During other radio observations the source went into undetectable levels in radio, below a few μJy. Only by stacking these other observations the source was detected again with a flux density of ~4 μJy. This proves the variability within the binary system and supports the possible variable gamma-ray emission as well, since it is related to changes in the accretion regime that could give rise to an increase in the acceleration of particles up to relativistic energies.

Aleksić et al. (2015) reported upper limits to the possible VHE emission of MWC 656 observed with the MAGIC telescopes. These upper limits are at the level of $2.0 \times 10^{-12}\,\mathrm{cm}^{-2}\,\mathrm{s}^{-1}$ and are not compatible with an extrapolation of the spectrum reported here up to TeV energies. This, however, does not exclude the possibility of VHE emission from MWC 656, since the MAGIC observations were carried out during a quiescent X-ray state of the binary, and VHE emission should not be expected during this state.

The accretion onto a BH in a system like MWC 656 might be explained by an advection dominated accretion flow (ADAF) (Narayan & Yi 1994). In this scenario, a very low accretion rate onto the compact object occurs, giving rise to very low X-ray emission. At radio wavelengths the source would display either a very low flux or it would not emit at all, as has been seen in Dzib et al. (2015), which reinforces the ADAF scenario. The radio emission could be interpreted as synchrotron radiation arising from a Comptonized environment of electrons near the BH. This population of electrons could be part of a corona and/or a non-already collimated jet.

In Cygnus X-3 the transient gamma-ray events occur during soft X-ray states or during transition states that precede major radio flares (Piano et al. 2012), while in Cygnus X-1 gamma-ray flares are more sporadic and were observed during hard states (Albert et al. 2007; Sabatini et al. 2010) or during hard-to-soft transitions (Sabatini et al. 2013). In the case of MWC 656 the source seems to be always in a quiescent state and the lack of simultaneous data during gamma-ray events prevent us from discussing the gamma-ray flares in relation to possible state transitions.

If coming from the binary, the gamma-ray flares could be produced within the Comptonized corona that surrounds the BH. In this case, relativistic electrons scatter soft photons either from the accretion disk or from the companion Be star. However, special conditions need to be fulfilled in order to give rise to the transient gamma-ray episodes. If coming from MWC 656, the gamma-ray luminosity of the 2010 event would be $L_\gamma = (9.0 \pm 5.2) \times 10^{35}\,\mathrm{erg\,cm}^{-2}\,\mathrm{s}^{-1}$, for a distance to the system of 2.6 ± 0.6 kpc.

6. CONCLUSIONS

In 2010 July *AGILE* detected the transient source AGL J2241+4454 which triggered the studies that revealed the first Be/BH binary system. Further searches in the *AGILE* data revealed that nine other flares from the same location occurred between 2008 and 2013 with energies above 100 MeV. By stacking all the detected events a spectral characterization of the source has been possible, yielding a fit to a power law with photon index $\Gamma = 2.3 \pm 0.2$ between 100 MeV and 3 GeV. The field around AGL J2241+4454 does not contain many possible counterpart sources. In fact we consider only two: RX J2243.1+4441, a radio galaxy with a possible FR-II type classification and thus less probable to be a gamma-ray emitter; and MWC 656, the above-mentioned HMXB containing a Be star and a BH. We consider the latter as the most suitable source to produce the observed gamma-ray emission, given its X-ray and radio characteristics. In order to do a more complete study, we confronted the *AGILE* data with *Fermi*/LAT data, performing the same study with both telescopes. However, the *Fermi*/LAT data do not show evidence of the observed gamma-ray emission. Nevertheless, we think that this might be due to differences in the way both telescopes observe, as well as to different energy-dependent sensitivity. Simultaneous radio to gamma-ray data in a wide temporal coverage is needed to unveil the identity of AGL J2241+4454.

APPENDIX
THE AGL J2241+4454 FIELD

In this Appendix we show the nearby X-ray sources that might be the counterpart of AGL J2241+4454 as well as the gamma-ray sources taken into account in the likelihood analysis which might be sources of contamination. Within the error box of the *AGILE* detection we find the two main candidates RX J2243.1+4441 and MWC 656. As explained in Section 2, there are two nearby gamma-ray sources that have been taken into account in the data analysis: 3FGL J2247.8+4413 which is a possible blazar located at ~9° from AGL J2241+4454, and 3FGL J2247.8+4413 a possible BL Lac object located at ~1° from AGL J2241+4454.

Table 2
AGL J2241+4454 Nearby Sources

Name	R.A. (h:m:s)	Decl. (°:′:″)	l (°)	b (°)	Distance to AGL J2241+4454 (°)	Notes
MWC 656	22:42:57.3	+44:43:18.3	100.1755	−12.3985	0.19	Be/BH binary system
RX J2243.1+4441	22:43:14.7	+44:42:31.0	100.2152	−12.4350	0.16	Possible FR-II Radio Galaxy
3FGL J2247.8+4413	22:47:53.2	+44:13:15.5	100.7236	−13.2583	0.93	Possible BL Lac
3FGL J2201.7+5047	22:01:44.2	+50:48:00.0	97.6417	−03.5460	9.24	Gamma-ray source
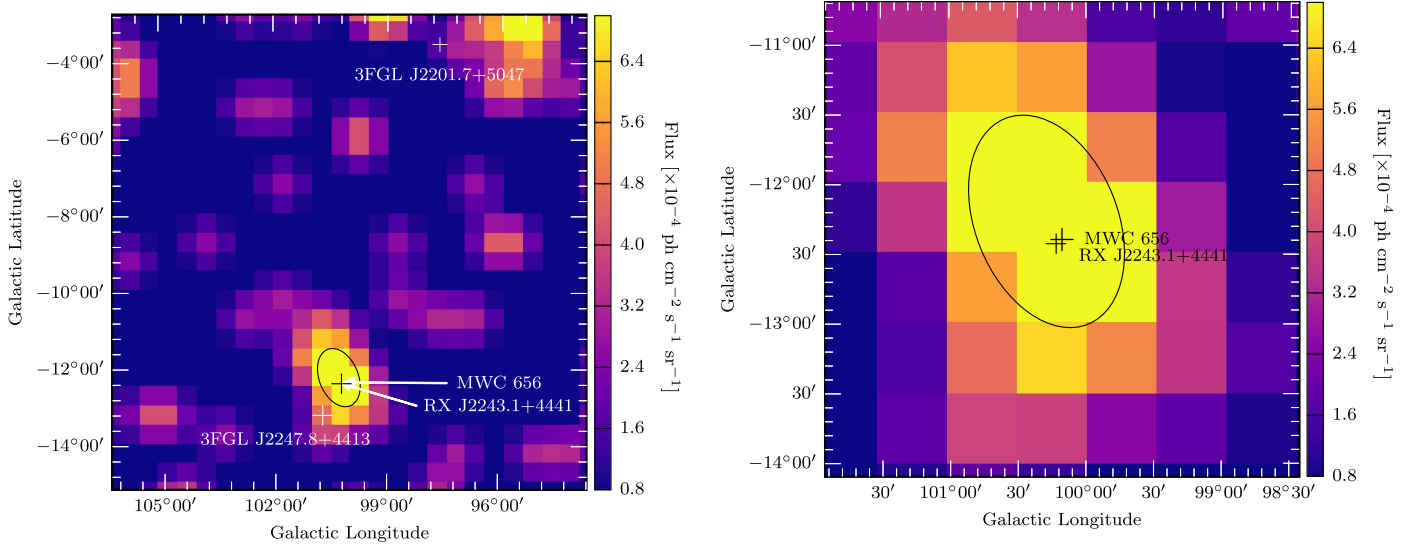
Figure 8. *AGILE* intensity map corresponding to the 2010 detected event. Left: the black ellipse corresponds to the 95% error box of the *AGILE* detection; within the error box there are MWC 656 and RX J2243.1+4441, which are very nearby. The source 3FGL J2201.7+5047 lies in the upper part of the map, while a possible BL Lac object, 3FGL J2247.8+4413, is located on the lower left part of the map. Right: zoom-in of the AGL J2241+4454 region and the sources inside the error box.

REFERENCES

Abdo, A. A., Ackermann, M., Ajello, M., et al. 2010, ApJ, 720, 912
Acero, F., Ackermann, M., Ajello, M., et al. 2015, ApJS, 218, 23
Ackermann, M., Ajello, M., Albert, A., et al. 2012, ApJS, 203, 4
Albert, J., Aliu, E., Anderhub, H., et al. 2007, ApJL, 665, L51
Aleksić, J., Ansoldi, S., Antonelli, L. A., et al. 2015, A&A, 576, A36
Alexander, M. J., & McSwain, M. V. 2015, MNRAS, 449, 1686
Barbiellini, G., Fedel, G., Liello, F., et al. 2002, NIMPA, 490, 146
Belczynski, K., & Ziolkowski, J. 2009, ApJ, 707, 870
Brinkmann, W., Siebert, J., Feigelson, E. D., et al. 1997, A&A, 323, 739
Bulgarelli, A., Chen, A. W., Tavani, M., et al. 2012, A&A, 540, A79
Casares, J., Negueruela, I., Ribó, M., et al. 2014, Natur, 505, 378
Casares, J., Ribó, M., Ribas, I., et al. 2012, MNRAS, 421, 1103
Chen, A. W., Argan, A., Bulgarelli, A., et al. 2012, Proc. SPIE, 8443, 4
Corbel, S., Coriat, M., Brocksopp, C., et al. 2013, MNRAS, 428, 2500
Dubus, G., Cerutti, B., & Henri, G. 2010, MNRAS, 404, L55
Dzib, S. A., Massi, M., & Jaron, F. 2015, A&A, 580, L6
Fender, R. 2010, in Lecture Notes in Physics, Vol. 794, ed. T. Belloni, (Berlin: Springer), 115
Fermi/LAT Collaboration, Abdo, A. A., Ackermann, M., et al. 2009, Sci, 326, 1512
Feroci, M., Costa, E., Soffitta, P., et al. 2007, NIMPA, 581, 728
Gallo, E., Fender, R. P., Miller-Jones, J. C. A., et al. 2006, MNRAS, 370, 1351
Gallo, E., Miller-Jones, J. C. A., Russell, D. M., et al. 2014, MNRAS, 445, 290
Grandi, P., Torresi, E., & Stanghellini, C. 2012, ApJL, 751, L3
Grudzinska, M., Belczynski, K., Casares, J., et al. 2015, MNRAS, 452, 2773

Hartman, R. C., Villata, M., Balonek, T. J., et al. 2001, ApJ, 558, 583
Hubert, A. M., & Floquet, M. 1998, A&A, 335, 565
Kiraga, M., & Stępień, K. 2013, AcA, 63, 53
Labanti, C., Argan, A., Bulgarelli, A., et al. 2006, NuPhS, 150, 34
Lucarelli, F., Verrecchia, F., Striani, E., et al. 2010, ATel, 2761, 1
Marcote, B. 2015, PhD thesis, Univ. de Barcelona
Mattox, J. R., Bertsch, D. L., Chiang, J., et al. 1996, ApJ, 461, 396
Munar-Adrover, P., Paredes, J. M., Ribó, M., et al. 2014, ApJL, 786, L11
Narayan, R., & Yi, I. 1994, ApJL, 428, L13
Paredes-Fortuny, X., Ribó, M., Fors, O., & Núñez, J. 2012, in AIP Conf. Ser. 1505, High Energy Gamma-Ray Astronomy, ed. F. A. Aharonian, W. Hofmann, & F. M. Rieger (Melville, NY: AIP), 390
Perotti, F., Fiorini, M., Incorvaia, S., Mattaini, E., & Sant'Ambrogio, E. 2006, NIMPA, 556, 228
Piano, G., Tavani, M., Vittorini, V., et al. 2012, A&A, 545, A110
Plotkin, R. M., Gallo, E., & Jonker, P. G. 2013, ApJ, 773, 59
Prest, M., Barbiellini, G., Bordignon, G., et al. 2003, NIMPA, 501, 280
Sabatini, S., Donnarumma, I., Tavani, M., et al. 2015, ApJ, 809, 60
Sabatini, S., Tavani, M., Coppi, P., et al. 2013, ApJ, 766, 83
Sabatini, S., Tavani, M., Striani, E., et al. 2010, ApJL, 712, L10
Sahakyan, N., Piano, G., & Tavani, M. 2014, ApJ, 780, 29
Sanchez, D. A., & Deil, C. 2013, arXiv:1307.4534
Tavani, M., Barbiellini, G., Argan, A., et al. 2008, NIMPA, 588, 52
Tavani, M., Bulgarelli, A., Piano, G., et al. 2009, Natur, 462, 620
van Leeuwen, F. 2007, A&A, 474, 653
Williams, S. J., Gies, D. R., Matson, R. A., et al. 2010, ApJL, 723, L93
Ziolkowski, J. 2014, AcPPP, 1, 175